q-PROFILE MEASUREMENTS IN THE CENTRAL PLASMA REGION OF ASDEX

K. McCormick, A. Eberhagen, H. Murmann and the ASDEX Team

MPIPP, EURATOM Association, Garching, FRG

Abstract: Using the Lithium-Beam-Spectroscopy (LBS) technique /1/ q-profile measurements have been carried out in the central region of diverted, ohmic ASDEX plasmas over a range $q(a)=2.9-5.3$ for $\bar{n}_e \sim 1\times10^{13}cm^{-3}$. The experimental results are consistent with a flat q(r) profile having $q(o)\sim1\pm0.06$ and exhibiting a slight tendency towards lower q(o) for decreasing q(a).

Motivation: Previous LBS measurements /2/ of q(o) in ASDEX for $q(a)\sim3.3$ gave $q(o)\sim1$ during ohmic heating. On TEXTOR $q(o)<1$ is measured over the range $q(a)=2.1-6.3$ /3/, whereas on TEXT q(o) is determined to be related to q(a), having $q(o)>1$ for large q(a) and vice versa.

In order to provide a broader data base for comparison with these findings, the LBS technique is used to investigate q(o) for a variety of q(a).

Experiment: The q(a) scan is performed in four discharge series whose parameters are listed in Table 1 along with the deduced q(o) values from neoclassical resistivity (NR) and LBS, as well as the sawtooth (ST) inversion radius r_{ST} from LBS, NR (here $r_{q=1}$ is equated to r_{ST}) and electron-cyclotron-emission (ECE). Three series have two I_p plateaus each, thereby enabling the relative $\Delta q(r)$ to be monitored more precisely since each plateau has a common measurement base line. The fourth series features a radial displacement of the plasma (R~166.5-163 cm) over 0.8 sec to achieve a moderate radial scan within one shot. Except for $q(a)=5.3$, where it is not certain, ST are present in all series with $\Delta Te_0/Te_0\sim5-8\%$. Series #1 is with hydrogen, the others with deuterium. Based on NR, $Z_{eff}\sim4-6$!

The density $\bar{n}_e$ of $\sim1\times10^{13}cm^{-3}$, plasma currents and toroidal fields chosen represent a balance between optimizing the LBS signal (low $\bar{n}_e$, high B_t) and the hindering of runaways (high $\bar{n}_e$, low I_p). Based on the gathered experience a larger q(a) range than covered here is accessible.

Results: The LBS technique measures the local magnetic field pitch angle $\theta_p=\tan^{-1}(B_p/B_t)$. Figure 1 illustrates the noise level and temporal behavior of $\theta_p(t)$ for series #1 at several values of the flux-surface radius r_f. The corresponding pitch angle θ_p^c profiles, adjusted to cylindrical geometry, are plotted in Fig. 4a; the values represent averages over 200 ms around the given time points, hence ST activity is completely averaged out. The representative error bar reflects the base line uncertainty (direction of $\vec{B}_t$) - accounting for ~2/3 of the total - and of θ_p^c itself.

Straight-line fits to the θ_p^c data in the central region, corresponding to a constant $q(=r_f/R\tan\theta_p^c)$, yield $q(o)\sim1.06$ and 0.95 for t=1 and 1.8 sec, respectively. Although neither Thomson scattering nor ECE profiles are available for corroborative evidence, the $r_f(q=1,\ t=1.8)\sim15.2$ cm value matches the $r_f(q=1)\geq1+a/q(a)$ $(1+40.2/2.93=14.7$ cm) scaling of the other series. By the same account, $r_f(q=1)$ for t=1 sec should be ~8.6 cm, meaning that only two measurement points are inside the expected q=1 surface, which is not adequate to characterize q(o).

The 2nd series was plagued with x-rays to the extent that no reasonably reliable θ_p measurement was possible. Nevertheless, the series serves to show that the $r_f(q=1)$ radius derived using neoclassical resistivity, under the assumption of a flat electric field- and Z_{eff}-profile, corresponds well with r_{ST}.

For the 3rd series, x-ray development again disturbed the diagnostic going into the second I_p plateau. Fig. 3 illustrates that up to this point, θ_p changes little in the inner region. The θ_p^c $(r_f,\ t=1.0)$ plot of Fig. 4b yields $q(r_f<9\text{ cm})\sim1.01\pm0.12$. For comparison, θ_p^c and q derived from neoclassical and Spitzer conductivity are also presented.

The typical broadening of the Te profile in response to a decrease in q(a) is demonstrated in Fig. 3a. Figure 3b serves both to convey an impression of the error bars on the Te-based calculation of θ_p^c over the series, as well as to confirm that a perceptible change in θ_p^c vs q(a) is to be expected only for $r_f>10$ cm.

The fourth series produced only a very marginal scan in r_f of ~0.6-1.1 cm due to the fact that θ_p is interrogated along a line inclined about 59° to the midplane. Nevertheless, θ_p^c $(r_f>4$ cm) in Fig. 4c is well documented: $q(r_f<11.2\text{ cm})\sim1.0^{+0.05}_{-0.04}$; $r_{ST}\sim12.1$ cm and $r_f(q=1)=12.9$ cm for neoclassical resistivity.

Discussion: Within this limited data base, varying q_a over 5.3-2.9 has ostensibly altered q(o) from ~1.06 to o.95. However, not enough radial points were present within the potential q=1 surface to convincingly describe q(o) for q(a)=5.3, and at q(a)=2.9 the uncertainty in θ_p^c encloses q(o)=1. One might fault the linear θ_p^c data fit within q=1; notwithstanding, a close examination of such furnishes no compelling motivation to introduce any other algorithm in the central region. Within any one series, local excursions of q(r) from the indicated value cannot be precluded, but may be regarded as unlikely when considering the overall direction of the results.

The experimental data are not consistent with the neoclassical prediction that q continues to monotonically decrease within $r_{q=1}$. On the other hand, the better agreement with the Spitzer profile is probably specious: Quite systematically - over a wider parameter range than presented here - Spitzer resistivity fails to correctly give r_{ST} and for low-q(a), sawtoothing discharges it often yields q(o)>1. In short, it is necessary to invoke neoclassical effects to approximately describe the experimental situation. The discrepancies within $r_{q=1}$ may be at least partially attributed to two effects: a) Due to the absence of points near the plasma center and the fit function chosen, the T_e profile is taken to be more peaked than in fact. (See Fig. 3a), b) The calculations assume a uniform E-field over the plasma cross section, which is known to be invalid in the presence of ST /5/.

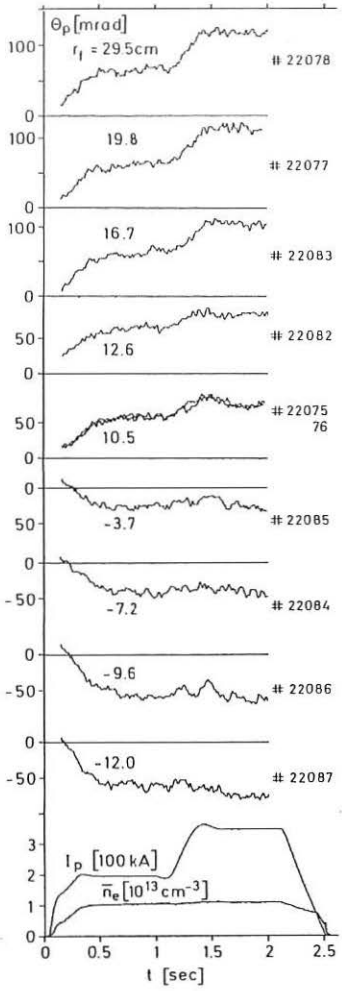

Fig. 1: Temporal behavior of the measured pitch angle θ_p, $\bar{n}_e$ and I_p for series # 1.

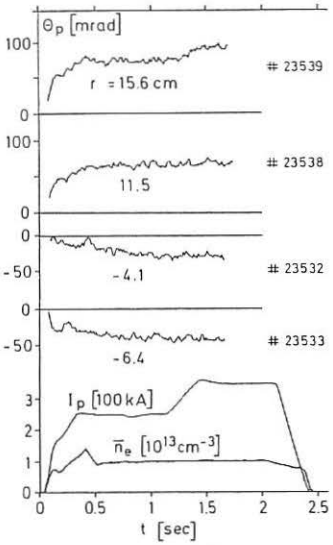

Fig. 2: $\theta_p(t)$, $\bar{n}_e$ and I_p for series # 3.

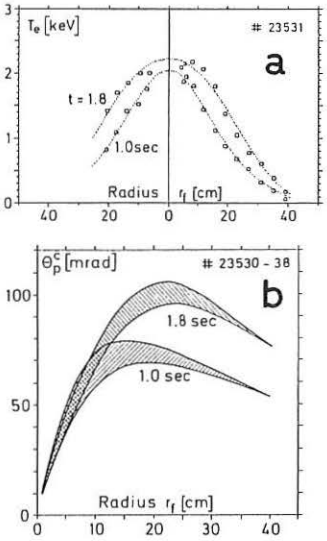

Fig. 3: (a) Te profiles from the YAG Thomson scattering system at t=1.0 and 1.8 sec for series # 3, (b) Pitch angle profiles derived from T_e profiles averaged over the series, assuming neoclassical resistivity.

Table 1: Experimental Parameters and Results

Series/Shot	B_t(kG)	I_p(kA)	q(a)	q(o) LBS	q(o) NR	r_{ST} LBS	r_{ST} NR	r_{ST} ECE
1: 22075-88	21	194	5.3	$1.06^{+0.8}_{-?}$	/	/	/	/
		348	2.93	0.95 ± 0.05	/	15.2	/	/
2: 22929-48	21.6	228	4.72	/	0.63	/	9.5	9.5
		348	3.06	/	0.67	/	13.7	14.0
3: 23524-39	23	249	4.55	1.01 ± 0.12	0.59	9	11.2	11.0
		348	3.22	/	0.65	/	13.6	13.8
4: 23634-44	22.8	299	3.77	$1.0^{+0.05}_{-0.04}$	0.62	11.2	12.9	12.2

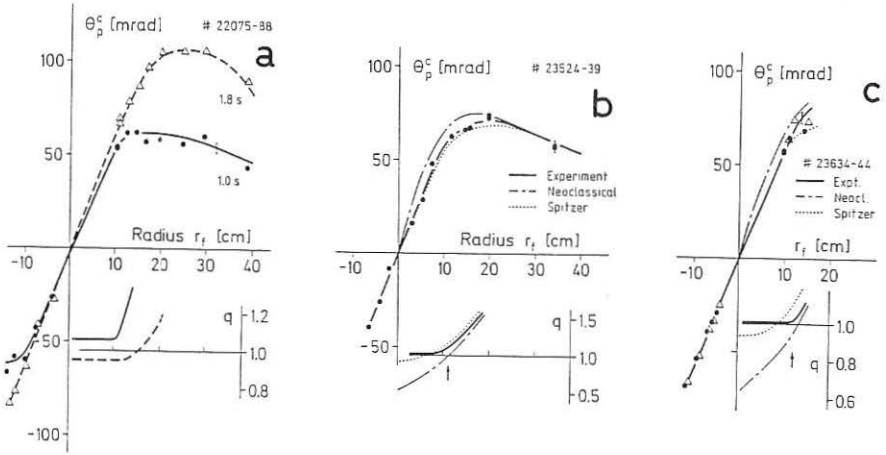

Fig. 4: Pitch angle profiles vs the flux surface radius r_f for: (a) first series, at t~1.0, 1.8 sec near the end of each I_p plateau. The corresponding $q(r_f)$ dependence derived from $q(r_f)=r_f/R\tan\theta_p^c$ is also given. (b) Third series, during the first plateau at t~1 sec; Comparison among the measured θ_p^c points and θ_p^c profiles based on neoclassical and Spitzer resistivity and associated q-profiles. The arrow indicates r_{ST} from ECE. (c) Fourth series: • R~166.5, △ R~163.9 cm.

References:

/1/ K. McCormick, Course on Diagnostic Techniques for Fusion Plasmas, Vol. II, (Varenna, 1986) 635.

/2/ K. McCormick, F.X. Söldner, et al., Proc. 13th EPS Conf., Vol. 2, (Schliersee, 1986) 323.

/3/ H. Soltwisch, H. Stodiek, et al., Proc. of the 11th IAEA Conf. on Plasma Physics and Controlled Fusion Research, Vol. 2, (Kyoto,1986) 263.

/4/ W.P. West, D. Thomas, et al., Phys. Rev. Lett. 58 (1987) 2758.

/5/ F. Alladio, et al., Proc 12th EPS Conf., Vol. 1, (Budapest, 1985) 138.